

DEVELOPMENT OF RISK EVALUATION METHOD CONSIDERING AFTERSHOCKS

*Seiichiro Fukushima¹, Hiroyuki Watabe² and Harumi Yashiro³

¹RKK Consulting Co., Ltd, Japan; ²Tokio Marine & Nichido Risk Consulting Co., Ltd, Japan;

³National Defense Academy, Japan

*Corresponding Author, Received: 30 Nov. 2018, Revised: 30 Dec. 2018, Accepted: 15 Jan. 2019

ABSTRACT: As shown in 2016 Kumamoto earthquake, it has become an issue that the damage or loss by aftershocks is greater than those by main shock. This situation is caused by the following two facts; the ground motion intensity by aftershocks are larger than that by main shock depending on the locations of aftershocks, and capacity of buildings is reduced by main shock. This paper proposes the methodology to probabilistically evaluate risks, such as loss or damage rate, considering the aftershocks. The methodology employed is the multi-event approach in which numerous events are generated with their location, shape, magnitude and occurrence probability so that the risk of not only a single building, but portfolio of buildings can be evaluated. This paper adds two features on the method; one is generating the conditional aftershock events, and the other is reducing the capacity of buildings reflecting damage status by main shock event. Model buildings located in the area where the effects of aftershocks cannot be ignored is used for application simulation with three conditions; no aftershocks, followed by aftershocks without capacity degradation, and followed by aftershocks with capacity degradation. The difference in the risks are evaluated by the risk curves. Through the simulation it is concluded that the proposed method can evaluate the risks considering aftershocks adequately.

Keywords: Aftershock, Risk evaluation, Seismic risk, Multi-event model, Risk curve

1. INTRODUCTION

Recently, it has become an issue that the damage or loss by aftershocks is greater than those by main shock. So, it is important for central and local government to evaluate risks not only by main shocks but also by aftershocks for adequate response against earthquakes. The above situation is caused by the following two facts; the ground motion intensity by aftershocks are larger than that by main shock depending on the locations of aftershocks, and capacity of buildings is reduced by main shock.

So far, some research regarding to aftershocks have been carried out as stated below.

- The Headquarters for Earthquake Research Promotion [1] proposed the probabilistic model of aftershock by combining the Gutenberg-Richter law and the modified Ohmori's formula, so that the probability of occurrence of aftershocks with given magnitude and within given period are obtained.
- Choi *et al.* [2] proposed the conditional seismic hazard analysis method of aftershocks for the effective response after large earthquakes. In the research authors examined the shape of source of aftershocks, their occurrence frequency, their maximum magnitude and so on based on the past earthquake data including 2011 Tohoku earthquake, Japan.
- Kumitani *et al.* [3] proposed the seismic source

of aftershocks as the function of the main shock. They also proposed the evaluation method of damage progress using Markov chain model.

- Miyakoshi *et al.* [4] proposed the generation of aftershock scenarios based on the past earthquake records, in which the magnitudes of series of aftershocks were modeled. They also examined the vulnerability functions of buildings damaged by main shocks.

Since probabilistic seismic risk analysis consists of seismic hazard analysis and fragility analysis, it may be concluded that basic components and basic concept for aftershocks have already provided.

The methodology employed is the multi-event model in which numerous events are generated with their location, shape, magnitude and occurrence frequency so that the risk of not only a single building, but portfolio of buildings can be evaluated. This paper adds two features on the method; one is generating the conditional aftershock events, and the other is reducing the capacity of buildings reflecting damage status by main shock event

2. SEISMIC HAZARD ANALYSIS

Generally, aftershocks are removed in the evaluation of seismic activity for the following reasons; aftershocks are dependent event of main shock and ground motions by aftershocks are assumed smaller than one by main shock. These reasons are adequate if aftershocks occur in the

vicinity of main shock. However as observed in some past earthquakes, the ground motion by aftershocks can be greater than one by main shock due to the location of site and seismic source.

2.1 Concept of Seismic Hazard Analysis

Seismic hazard is evaluated by combining the seismic hazard by main shock and one by aftershocks. The concept of seismic hazard analysis for a given main shock is introduced in order to facilitate explanation. It is noted that ground motion measure employed is the peak ground velocity (hereinafter referred as PGV) unless otherwise noted.

2.1.1 Seismic Hazard by A Given Main Shock

Let v_m , \bar{x}_m and ζ_m be annual occurrence frequency, median of PGV and log normal standard deviation of PGV, respectively. The annual frequency $v(x_m > y)$ that PGV by main shock x_m exceeds the given threshold y is obtained by Eq. (1).

$$v(x_m > y) = v_m \cdot \left[1 - \Phi \left(\frac{\ln(y/\bar{x}_m)}{\zeta_m} \right) \right] \quad (1)$$

The annual probability $p(x_m > y)$ that PGV by main shock exceeds the given threshold is obtained by Eq. (2)

$$p(x_m > y) = 1 - \exp[-v(x_m > y)] \quad (2)$$

2.1.2 Seismic hazard by aftershocks

Aftershocks are modeled as background earthquakes, whose activity is given by Gutenberg-Richter's (hereinafter G-R's) formula. Let j and $v_{j|m}$ be the index of j^{th} aftershock and conditional frequency, respectively. The conditional frequency $v_c(x_j > y)$ that PGV by j^{th} aftershock x_j exceeds the given threshold y is obtained by Eq. (3).

$$v_c(x_j > y) = v_{j|m} \cdot \left[1 - \Phi \left(\frac{\ln(y/\bar{x}_j)}{\zeta_j} \right) \right] \quad (3)$$

Therefore, the conditional frequency $v_c(x_A > y)$ that PGV by aftershocks exceeds the given threshold is obtained by Eq. (4).

$$v_c(x_A > y) = \sum_{j=1}^n \left[v_{j|m} \cdot \left[1 - \Phi \left(\frac{\ln(y/\bar{x}_j)}{\zeta_j} \right) \right] \right] \quad (4)$$

The conditional probability $p_c(x_A > y)$ that PGV by aftershocks exceeds the given threshold is obtained by Eq. (5).

$$p_c(x_A > y) = 1 - \exp[-v_c(x_A > y)] \quad (5)$$

Finally, unconditional probability $p(x_A > y)$ that PGV by aftershocks exceeds the given threshold is obtained by multiplying the occurrence probability of main shock as shown by Eq. (6).

$$p(x_A > y) = [1 - \exp(-v_m)] \cdot p_c(x_A > y) \quad (6)$$

2.1.3 Integration of seismic hazards by main shock and aftershock

Since aftershocks are dependent event of main shock, Eq. (7) is employed to integrate the hazards by main shock and aftershocks.

$$p(x > y) = \max[p(x_m > y), p(x_A > y)] \quad (7)$$

2.2 Modeling of Aftershocks

As mentioned above, aftershocks are modeled as background earthquakes. Condition setting is based on [2].

2.2.1 Location of Aftershocks

Aftershocks are assumed to occur uniformly in the region whose area A_a is given by Eq. (8) with the magnitude of main shock M_m .

$$A_a = 10^{0.778M_m - 1.60} \quad (8)$$

2.2.2 Maximum magnitude of aftershocks

The maximum magnitude of aftershocks is given by Eq. (9) with the magnitude of main shock M_m .

$$M_a = M_m - 1.0 \quad (9)$$

2.2.3 Seismic activity of aftershocks

Let M_m and T_1 be the magnitude of main shock and elapsed time in day, respectively. The number of aftershocks is given by Eq. (10).

$$N(T_1, M_m) = 10^{0.88M_m - 4.51} \frac{(T_1 + c)^{1-p} - c^{1-p}}{(90 + c)^{1-p} - c^{1-p}} \quad (10)$$

Parameters p and c are constants in modified Omori formula described in [2]. This paper employs 1.05 for p and 0.1 for c . b -value in G-R's formula is set 0.83.

2.3 Application

The model site is shown in Fig. 1. The site is considered to be affected by large earthquakes with high potential of generating aftershocks.

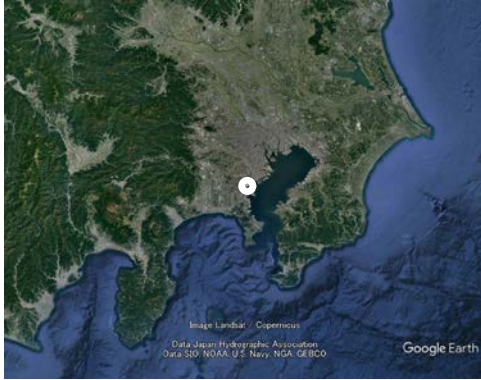


Fig.1 Location of model site

2.3.1 Seismic source model

For the purpose of accountability, seismic sources were modeled based on the database used in “Japan Seismic Hazard Information Station”, in which Poisson’s process was employed. Aftershocks were modeled in accordance with the policy.

2.3.2 Ground Motion Prediction Equation

Ground motion prediction equation used in [5] was employed in the analysis. Equation (11) shows the attenuation formula for PGV.

$$\log PGV = \begin{cases} a_1 M_w + b_1 X - \log(X + d_1 \cdot 10^{0.5 M_w}) - c_1 & (11) \\ a_2 M_w + b_2 X - \log(X) - c_2 \end{cases}$$

- PGV : peak ground velocity
- M_w : moment magnitude
- X : shortest distance
- D : focal depth
- a_1, b_1, c_1, d_1 : coefficients ($D \leq 30$)
- a_2, b_2, c_2 : coefficients ($D > 30$)

Correction factor G for ground motion by surface layer was also calculated by Eq. (12),

$$G = p \log(vs) + q \quad (12)$$

where, p and q are regression coefficients, and vs is the mean shear wave velocity of surface soil to a depth of 30 m.

2.3.3 Results

The probabilistic hazard curves at model site is shown in Fig. 2, from which it can be seen that the contribution of aftershocks appears in the range of low exceedance probability since the aftershocks are dependent events of huge earthquakes with small occurrence probability. On the contrary, the contribution in the range of high exceedance probability is negligible. It is also observed that the PGV by aftershocks is greater than that by main

shock in the range of extremely low exceedance probability.

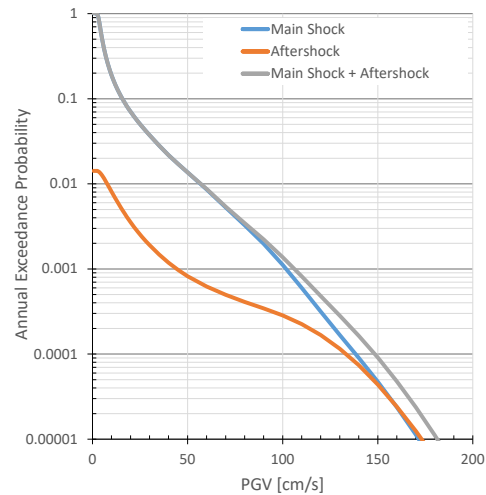


Fig.2 Seismic hazard curve at model site

3. SEISMIC FRAGILITY ANALYSIS

In risk evaluation considering aftershocks it is necessary to take the damage by main shock into account. For that purpose, this paper proposes the modification of damage function (hereinafter called DF) that is the relationship between ground motion intensity and damage ratio according to the damage by main shock.

3.1 Basic Idea of Modification of DF

Let x and $R_m(x)$ be PGV and DF for main shock, respectively. Two ways to modify DF can be considered; one is to adjust PGV, and the other is to adjust damage ratio. This paper employs the former way because of the following reasons; the damage ratio possesses the upper and lower limits so that multiplying a constant may bring the inadequate damage ratio. Therefore, change of DF is caused by the reduction in median capacity velocities of fragility curves by damage.

Let $R_a(x)$ be DF for aftershocks. This paper assumes that $R_a(x)$ can be calculated by Eq. (13).

$$R_a(x) = R_m(k_D(r) \cdot x) \quad (13)$$

$k_D(r)$ is the factor to adjust PGV according to the damage ratio r by main shock. It is noted that $k_D(r)$ equal to or greater than unity. In this paper $k_D(r)$ is referred to as DF modification factor. One advantage to employ the DF modification factor is that the DF for main shock can be used for aftershocks with no modification.

3.2 Evaluation of DF Modification Factor

DF modification factor was evaluated statistically using the results of numerical calculations, in which eight model buildings (two structural types times four types of stories) converted into SDOF system were employed.

Fukushima *et al.* [6] gives more detailed explanation on the simulation method.

3.2.1 Seismic Capacity of Buildings

Seismic capacity of each building was expressed by the tri-linear skeleton curve of equivalent SDOF model, whose characteristics were summarized in Tables 1 and 2.

Table 1 Parameter for skeleton curves (before main shock)

Parameters	Setting policy
Initial Stiffness	$k_0 = m \left(\frac{2\pi}{T} \right)^2$
Stiffness after cracking	$k_1 = \frac{k_0}{3}$
Stiffness after yielding	$k_2 = 0$
Cracking strength	$s_1 = \frac{s_2}{3}$
Yielding strength	$s_2 = 1.2 \times s_d$

m : mass
 T : natural period
 s_d : design capacity

Table 2 Parameter for skeleton curves (after main shock)

Parameters	Setting policy
Initial Stiffness	k'_0 : secant stiffness corresponding to damage
Stiffness after cracking	$k'_1 = k_1$, if $d'_c \leq d'_y$ $k'_1 = 0$, if $d'_c > d'_y$
Stiffness after yielding	$k'_2 = 0$
Cracking strength	$s'_1 = \alpha \cdot s_1$
Yielding strength	$s'_2 = \alpha \cdot s_2$

d'_c : cracking displacement
 d'_y : yielding displacement
 α : strength reduction factor

Table 3 summarizes the drift angle to estimate displacement and strength reduction factor for each damage level. Drift angles for given damage states were given based on the existing research and strength reduction factors were estimated based on [7] that describes the method on seismic diagnosis.

Table 3 Reference drift angle and strength reduction factor

Damage	Drift angle		Strength reduction factor
	RC	S	
No	-	-	1.00
Damage Slight	1/240	1/160	1.00
Moderate	1/120	1/80	0.95
Severe	1/60	1/40	0.90
Collapse	1/30	1/20	0.80

Equivalent building height to calculate the displacement of SDOF system H_r was calculated by Eq. (14), where H is the building height.

$$H_r = \frac{2n + 1}{3n} H \quad (14)$$

Examples of skeleton curves of SDOF systems that correspond to RC-8 story building and S-8 story are shown in Fig. 3, in which legend shows the damage by main shock. It is noted that the strength is given by response acceleration instead of story shear force. From the figure it can be seen that capacity of buildings will be largely reduced if buildings reach to the severe damage by main shock.

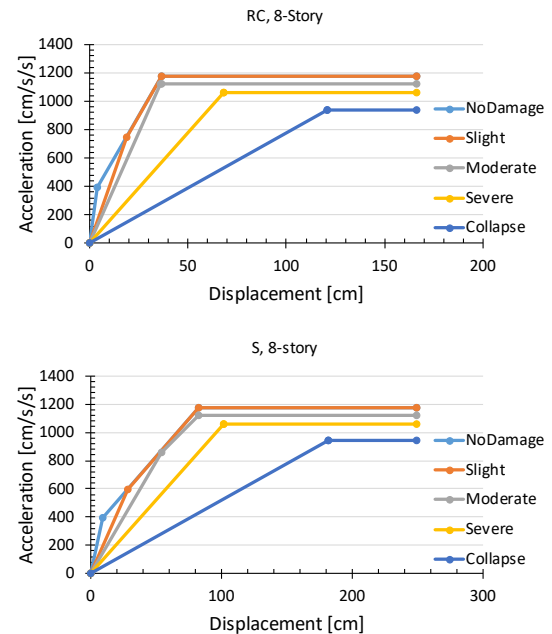


Fig.3 Examples of skeleton curves subject to main shock

3.2.2 Change of capacity velocity after main shock

In this paper, response of SDOF system was obtained as the inter section of capacity spectra whose samples are shown in Fig.3 and demand spectrum shown in Fig. 4. This demand spectrum

was selected as standard soil, whose magnitude is dependent of ductility factor of SDOF system.

Since capacity spectrum method cannot evaluate velocity that bring the buildings to given damage state, this paper assumed that the reduction of demand spectrum that cause the buildings damage is proportional to the reduction of capacity velocity.

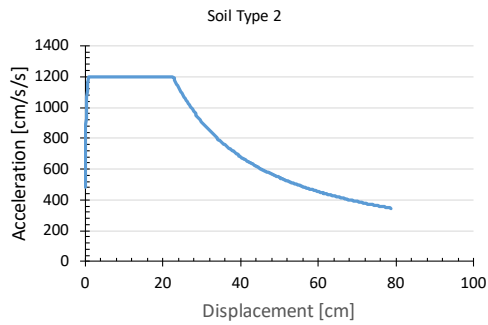


Fig.4 Demand spectrum used in the analysis

Examples of reduction of demand spectrum for two sample buildings are shown in Fig. 5, in which the reduction is given by the ratio of the magnitude of demand spectrum. It is noted that the damage ratios for “slight”, “moderate”, “severe” and “collapse” were set 0.025, 0.075, 0.2 and 0.65, respectively.

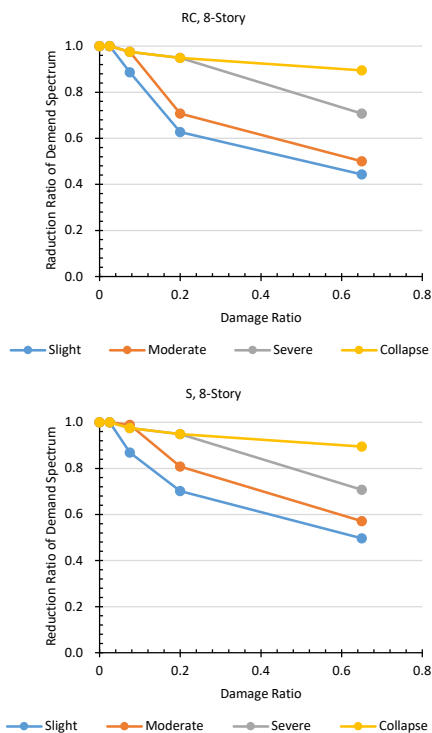


Fig.5 Example of reduction of demand spectrum

3.2.3 Regression of reduction ratio

In addition to the reduction ratios shown in Fig. 5, other ratios for buildings of three, five and twelve stories were calculated for regression analysis in parameter r , which is the damage ratio by main shock.

Figure 6 shows the average relationship between damage ratio and reduction ratio of demand spectrum, in which it can be seen there is little difference about structural type. Therefore, regression analysis was done regardless of structural type.

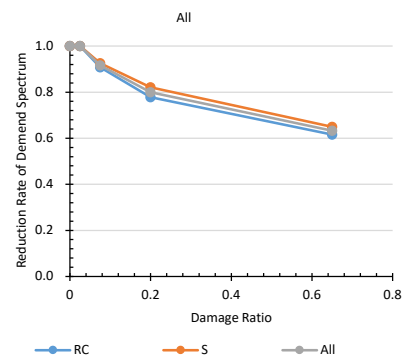


Fig.6 Reduction of demand spectrum

Let r and y be damage ratio and reduction ratio of demand spectrum, respectively. Considering the shape of curve in Fig. 7, the following equation was obtained by the regression analysis.

$$y = \min[-0.114 \ln(r) + 0.6007, 1.0] \quad (15)$$

The DF modification factor $k_D(r)$ is given as a reciprocal of Eq. (15) as follows.

$$k_D(r) = \max\left[\frac{1}{0.6007 - 0.114 \ln(r)}, 1.0\right] \quad (16)$$

4. SEISMIC RISK ANALYSIS FOR SINGLE BUILDING

As risk analysis, this paper evaluates event risk curve which is the relationship between the damage and its annual exceedance probability. It is noted that the risk of concern is the 90th percentile value of damage ratio derived from probabilistic distribution function of damage ratio of each event.

The concrete procedures are illustrated in [8-10].

4.1 Probability Distribution Function of Damage Ratio

Probability distribution function of damage ratio is evaluated by Monte Carlo simulation. Followings are explanations of evaluation of damage ratio for a

given Monte Carlo trial.

Let x_i and $R_i(x_i)$ be PGV at site and damage ratio by i^{th} main shock, respectively. Then, let x_j be PGV at site by j^{th} aftershock that is dependent event of main shock. The damage ratio by j^{th} aftershock is given by $R_j(k_D(r) \cdot x_j)$, where $k_D(r)$ is the DF modification factor mentioned before.

Let n_i and v_j be the number of aftershocks and the conditional occurrence frequency, respectively. And, let R_i and R_j be damage ratios by main shock and j^{th} aftershock for simplicity. The composite damage ratio \hat{R}_i is calculated by Eq. (17). In case when no aftershock occurs or damage ratio by aftershocks are negligible, \hat{R}_i and R_i are identical.

$$\hat{R}_i = 1 - (1 - R_i) \cdot \prod_{j=1}^{n_i} (1 - R_j)^{v_j} \quad (17)$$

4.2 Condition Setting for Analysis

Four DFs shown in Fig.7 were employed to investigate the effect of the difference in DFs on the event risk curves.

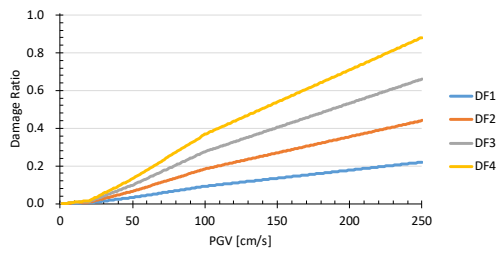


Fig.7 Damage functions used for risk evaluation

Also, three analysis cases were introduced as follows.

- Case-1: No aftershocks occur.
- Case-2: Aftershocks occur.
Building's capacity is decreased.
- Case-3: Aftershocks occur.
Building's capacity is not decreased.

4.3 Evaluation of Event Risk Curves

Evaluated event risk curves are shown in Fig. 8.

Since aftershocks are dependent event of main shock, their effect on the risk curve does not appear in the range of high occurrence probability. And, even though in the low occurrence probability range, DF1 and DF2 do not bring the effect of aftershocks, since damage ratios by main shock are negligible. On the contrary, DF3 and DF4 bring the effect of aftershocks due to the reduction of building's capacity by main shock.

It is noted that DF3 and DF4 bring the effect of

aftershocks in Case-2 though no capacity reduction exists. This may be caused by the increment of PGV by aftershocks.

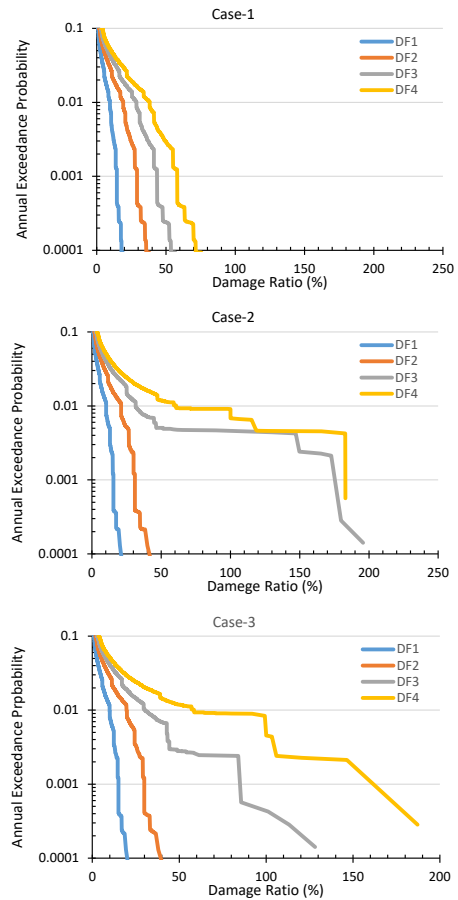


Fig.8 Comparison of event risk curves

5. SEISMIC RISK ANALYSIS FOR PORTFOLIO OF BUILDINGS

5.1 Condition Setting

As an application, employed is a portfolio consisting of three facilities in Kanto region where large scale earthquakes with aftershocks hit. The location of facilities is shown in Fig. 9. The figures in parenthesis are amplification factor of surface layer. The seismic capacity of each facility is assumed identical. Their damage functions are DF1 in Fig.7. Price of each building is set 100.

Seismic source model and ground motion prediction equation are the same as ones used in the previous chapters.

Three analysis cases are also employed.

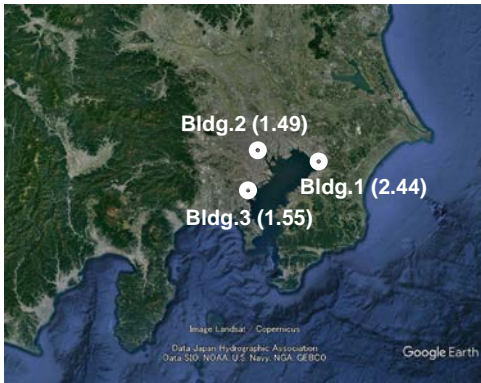


Fig.9 Location of buildings forming portfolio

5.2 Evaluation of Event Risk Curves

Based on the conditions described above, the event risk curves were obtained as shown in Fig. 10, where damage functions of portfolio and of each facility are given simultaneously.

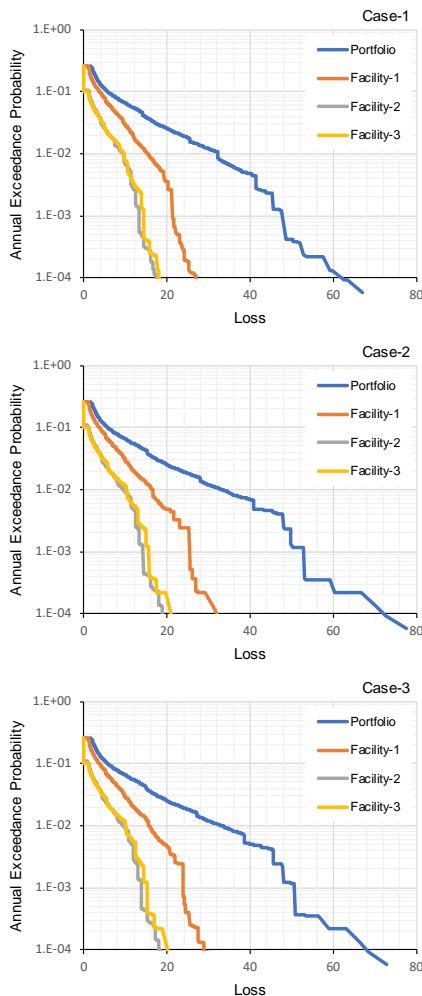


Fig.10 Comparison of event risk curves

From the figures, it can be seen that contribution of building 3 to the portfolio risk is high due to large ground motion amplification factor. It is also apparent that the effect of aftershocks on event risk curve appears in the range of low exceedance probability, since aftershocks are dependent event of large earthquakes whose occurrence probabilities are small.

Figure 11 compares the event risk curves of portfolio by analysis cases. As described above, the effect of aftershocks appears in the range that annual exceedance probability is 0.01 or smaller. The deference between Case-1 and Case-3 is given by the reduction in capacity of facilities, and the deference between Case-2 and Case-3 is by the increment of seismic hazard. Therefore, it can be seen two effects of aftershocks on event risk curve are more or less equal within the limit of simulation.

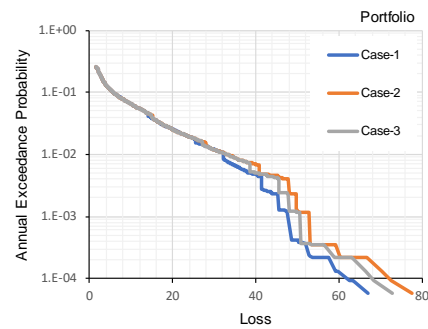


Fig.11 Comparison of event curve by analysis cases

Table 4 summarizes the loss ratios of portfolio at given annual exceedance probabilities, where loss ratio is defined as the ratio of loss of given analysis case to the one of Case-1. From the loss ratios in the table it can also be concluded that the effects of aftershocks on the event risk curves appear in the low probability range as explained above.

Table 4 Comparison of ross ratios at given annual exceedance probabilities

Annual Exceedance probability	Loss ratio (to Case-1)		
	Case-1	Case-2	Case-3
1/50	1.00	1.00	1.00
1/100	1.00	1.03	1.03
1/200	1.00	1.05	1.04
1/500	1.00	1.10	1.06
1/1000	1.00	1.11	1.06

6. CONCLUSIONS

This paper adds two features on the existing risk evaluation method; one is increasing ground motion

intensity by the generated conditional aftershock events, and the other is reducing the capacity of buildings reflecting damage status by main shock event. Through the simulation it is found that the effects of the added features duly appear as the change of event risk curves.

In 1995 Hyogo-ken Nambu earthquake (Kobe earthquake) it was pointed out that buildings designed and constructed after 1981 could withstand the ground motion intensity of 7 in JMA scale corresponding 10 to 12 in MMI scale. However, some of such buildings could not withstand the series of the ground motion intensity of 7 as shown in 2016 Kumamoto earthquake. One of the reasons is that buildings damaged by the mainshock could not withstand the second large ground motion. So, it can be said that the tendency observed in the application study is compatible to the damage situations in past earthquakes.

This method will be applied to the large active fault as next step.

7. ACKNOWLEDGEMENTS

Authors give great thanks to Mr. Hayashi from Tokio Marine & Nichido Risk Consulting Co., Ltd. for his effort in providing database of aftershocks regarding to large inter-plate earthquake around Japan islands

8. REFERENCES

- [1] The Headquarters for Earthquake Research Promotion, On probabilistic evaluation method, “<http://www.jishin.go.jp/main/yoshin2/yoshin2.htm>”, (in Japanese)
- [2] Choi B., Itoi T., Takada T., Probabilistic aftershock occurrence model and hazard assessment for post-earthquake restoration activity plan, J. Struct. Constr. Eng., AIJ, Vol.78 No.690, 2013, pp.1377-1383, (in Japanese)
- [3] Kunitani S., Takada T., “Probabilistic assessment of buildings damage considering aftershocks of earthquakes”, J. Struct. Constr. Eng., AIJ, Vol.74 No.637, 2009, pp.459-465, (in Japanese).
- [4] Miyakoshi J., Ju D., Shimazu N, Kambara H. Yamada K., “Prediction of building damage considering main shock and aftershocks: part 1-3”, Transaction of AIJ, 2010, pp.1061-1066, (in Japanese).
- [5] National Research Institute for Earth Science and Disaster Resilience, Technical Note of the National Research Institute for Earth Science and Disaster Resilience, No. 336.
- [6] Fukushima S., Watabe H., Yashiro H., Development of Risk Evaluation Method Considering Aftershocks, Proc of 7th Asia Conference in Earthquake Engineering, Paper ID 0080, 2018.
- [7] Japan Building Disaster Prevention Association, Standard for seismic evaluation of existing reinforced concrete buildings, 2001, (in Japanese).
- [8] Fukushima S., Yashiro H., Seismic risk analysis on portfolio of buildings, J. Archit. Plann. Environ. Eng., AIJ, No.552, 2002, pp.169-176, (in Japanese)
- [9] Fukushima S., Yashiro H., An analysis for condition settings in securitizing seismic risk, J. Archit. Plann. Environ. Eng., AIJ, No.555, 2002, pp.295-302, (in Japanese)
- [10] Fukushima S., Yashiro H., Seismic performance level of buildings considering risk transfer, J. Struct. Constr. Eng., AIJ, No.567, 2003, pp.197-204, (in Japanese)